Food Chemistry 152 (2014) 251–260

Contents lists available at ScienceDirect

Food Chemistry

journal homepage: www.elsevier.com/locate/foodchem

In vitro evaluation method for screening of candidate prebiotic foods

Yasuhiro Date [a,b], Yumiko Nakanishi [b,1], Shinji Fukuda [b,c,1], Yumi Nuijima [b], Tamotsu Kato [c], Mikihisa Umehara [a,2], Hiroshi Ohno [b,c], Jun Kikuchi [a,b,d,e,*]

[a] *RIKEN Center for Sustainable Resource Science, 1-7-22 Suehirocho, Tsurumi-ku, Yokohama, Kanagawa 230-0045, Japan*
[b] *Graduate School of Medical Life Science, Yokohama City University, 1-7-29 Suehirocho, Tsurumi-ku, Yokohama, Kanagawa 230-0045, Japan*
[c] *RIKEN Center for Integrative Medical Sciences, 1-7-22 Suehirocho, Tsurumi-ku, Yokohama, Kanagawa 230-0045, Japan*
[d] *Graduate School of Bioagricultural Sciences, Nagoya University, 1 Furo-cho, Chikusa-ku, Nagoya, Aichi 464-0810, Japan*
[e] *Biomass Engineering Program, RIKEN Research Cluster for Innovation, 1-7-22 Suehirocho, Tsurumi-ku, Yokohama, Kanagawa 230-0045, Japan*

ARTICLE INFO

Article history:
Received 23 June 2013
Received in revised form 18 November 2013
Accepted 22 November 2013
Available online 1 December 2013

Keywords:
NMR
Multivariate statistical analysis
Metabonomics
Microbiota
Welsh onion

ABSTRACT

The aim of this work was to develop a simple and rapid *in vitro* evaluation method for screening and discovery of uncharacterised and untapped prebiotic foods. Using a NMR-based metabolomic approach coupled with multivariate statistical analysis, the metabolic profiles generated by intestinal microbiota after *in vitro* incubation with feces were examined. The viscous substances of Japanese bunching onion (JBO_{VS}) were identified as one of the candidate prebiotic foods by this *in vitro* screening method. The JBO_{VS} were primarily composed of sugar components, especially fructose-based carbohydrates. Our results suggested that ingestion of JBO_{VS} contributed to lactate and acetate production by the intestinal microbiota, and were accompanied by an increase in the *Lactobacillus murinus* and *Bacteroidetes* sp. populations in the intestine and fluctuation of the host-microbial co-metabolic process. Therefore, our approach should be useful as a rapid and simple screening tool for potential prebiotic foods.

1. Introduction

The co-evolution of mammalian-microbial symbiosis is accompanied by extensive interactive modulations of metabolism and physiology, facilitated by the crosstalk between the host and symbiotic community. Microbial symbionts often provide traits that their hosts have not evolved on their own, and may synthesise essential amino acids and vitamins or process otherwise indigestible components in the diet, such as plant polysaccharides (Flint, Bayer, Rincon, Lamed, & White, 2008; Turnbaugh et al., 2007). The composition of intestinal microbial communities is highly variable (Turnbaugh et al., 2007), and can be significantly affected by alterations in diet (Flint et al., 2008). Interactive modulations of individuals with variations in their microbial symbionts are likely to affect human health and disease (Turnbaugh et al., 2007).

The interactive modulations affecting human health are considerably engaged by beneficial microbial symbionts such as *Lactobacilli* and *Bifidobacteria*, which are currently the most marketed probiotic bacteria worldwide (Saulnier, Spinler, Gibson, & Versalovic, 2009). The beneficial microbial symbionts are responsible for preventing infection, enhancing the immune system, and providing increased nutritional value to food (Fukuda et al., 2011; Saulnier et al., 2009; Ventura et al., 2009). The growth and activity of these beneficial microbial symbionts is enhanced by prebiotic foods, such as fructo-oligosaccharide (FOS) and galacto-oligosaccharides, in the human gastrointestinal tract (Saulnier et al., 2009). Therefore, evaluation of the effects of prebiotic foods on the dietary interactive modulations of the host and the beneficial microbial symbionts are important for human health.

Some foods and their components are customarily considered to play an important role in human health. For example, Japanese bunching onion (JBO) (synonym for welsh onion; *Allium fistulosum* L.), an edible perennial plant, is considered to be beneficial for human health in Japan. The edible portions of the JBO are the green stalk and the white bulb, which are used as ingredients in Asian cuisine, especially in East and Southeast Asia. The edible portion of JBO has been reported to show hypolipidemic effects (Yamamoto, Aoyama, Hamaguchi, & Rhi, 2005), antioxidant effects in rats fed

* Corresponding author at: RIKEN Center for Sustainable Resource Science, 1-7-22 Suehirocho, Tsurumi-ku, Yokohama, Kanagawa 230-0045, Japan. Tel.: +81 455039439; fax: +81 455039489.
E-mail address: jun.kikuchi@riken.jp (J. Kikuchi).
[1] Present address: Institute for Advanced Biosciences, Keio University, 246-2 Kakuganji, Mizukami, Tsuruoka, Yamagata 997-0052, Japan.
[2] Present address: Department of Applied Biosciences, Faculty of Life Sciences, Toyo University, 1-1-1 Izumino, Itakura-machi, Ora-gun, Gumma 374-0193, Japan.

0308-8146
http://dx.doi.org/10.1016/j.foodchem.2013.11.126

a high-fat and high-sucrose diet (Yamamoto & Yasuoka, 2010), and hypoglycemic effects in an animal model of diabetes mellitus (Kang et al., 2010). In addition, the JBO is customarily considered a preventative food against the common cold and influenza in Japan. In support of this, a recent study reported that the macromolecular component obtained by aqueous solvent extraction of JBO had anti-influenza activity (Lee et al., 2012). However, viscous substances (VS), a macromolecular component extractable by aqueous solvent and produced in the cavity of JBO (JBO_{VS}), are not well-characterized with regard to their chemical and mineral compositions. Moreover, limited biological information about the effects of the JBO_{VS} on host-microbial symbiotic systems in the intestines is available. Thus, a large number of foods and their components derived from plants such as JBO_{VS} may have undiscovered human health benefits.

Candidate functional and prebiotic foods are usually evaluated using *in vitro* cell assays and/or animal experiments in mice and rats. Animal experiments, however, are generally time-consuming and present several ethical issues. With this in mind, it was envisaged that a simple and rapid *in vitro* method involving the use of *in vitro* cell assays would be a much more suitable method for the screening of functional and prebiotic foods. Therefore the objective of this study was to develop a simple and rapid *in vitro* evaluation method for screening and discovery of uncharacterised and untapped prebiotic foods. To accomplish this objective, a metabolomic approach was employed, which is a powerful tool well suited to provide metabolic profiles that contain information pertaining to the ecosystem and community response. Multivariate metabolic profiling offers a practical approach for measuring the metabolic endpoints that are directly linked to whole system activity (Nicholson, Holmes, & Wilson, 2005). In addition to this, some approaches, including our developed methods, have been successfully applied to characterising the metabolic consequences of nutritional intervention, monitoring the metabolic dynamics in microbial ecosystems, and linking the relationships between microbial communities and their metabolic information (Date et al., 2010; Li et al., 2008; Rezzi, Ramadan, Fay, & Kochhar, 2007).

Herein we describe an *in vitro* evaluation method for a rapid and simple screening of candidate prebiotic foods and their components. The JBO_{VS} and other foods and their components were evaluated by an *in vitro* screening method based on the metabolic dynamics of microbial communities obtained by nuclear magnetic resonance (NMR) spectroscopy and denaturing gradient gel electrophoresis (DGGE) fingerprinting. In addition, we characterised the chemical components in the JBO_{VS} by NMR spectroscopy and inductively coupled plasma optical emission spectrometry (ICP-OES)/mass spectrometry (ICP-MS) analysis. Furthermore, the effects of the JBO_{VS} observed by *in vitro* screening were evaluated on the host-microbial symbiotic system in the intestines by an approach based on metabolic and microbial community profiles obtained by NMR spectroscopy and DGGE fingerprinting, respectively.

2. Materials and methods

2.1. Materials

The materials used in a screening method were as follows: FOS from chicory, raffinose, stachyose, pectin from apple, wheat-bran, carrageenan (Sigma-Aldrich Japan Co., Ltd., Tokyo, Japan), chlorella (Chlorella Industry Co., Ltd., Tokyo, Japan), starch from wheat, glucan, agar (Wako Pure Chemical Industries, Ltd., Osaka, Japan), onion, kelp, Japanese mustard spinach, arrowroot, starch from arrowroot (purchased from a market), JBO, and JBO_{VS}. The variety of JBO used in this study was Fuyuougi 2. The JBOs themselves were obtained from the Kanagawa Agricultural Technology Center (Kanagawa, Japan). The JBOs were planted in soil taken from the farm at the Center for about 3 months at the mature stage, and the resulting JBO_{VS} were collected from the JBO cavity when the JBO was harvested.

2.2. In vitro incubation

Male 10-week-old BALB/cA mice (CLEA Japan, Inc., Tokyo, Japan) were housed at 23–25 °C and 50–60% relative humidity with a 12 h light-dark cycle. The mice were fed CLEA Rodent Diet CA-1 (CLEA Japan, Inc., Tokyo, Japan). Fresh fecal sources were collected from the mice. The collected fecal sources (1%) were suspended anaerobically in phosphate-buffered saline (PBS) (8 g NaCl, 0.2 g KCl, 2.9 g $Na_2HPO_4{\cdot}12H_2O$, and 0.2 g KH_2PO_4 per litre distilled water, pH 7.0) with 0.5% (w/v) of each substrate. The PBS solutions containing 5 mg/L resazurin and 1 mg/L cysteine hydrochloride were used to provide an indication of the amount of oxygen in the medium and act as an oxygen scavenger, respectively. These solutions were pretreated with pure CO_2 (>99.9%) gas and autoclaved before being mixed with the fecal sources. The substrates examined were from the above-mentioned list of materials, as well as a control (no addition of substrate). All substrates were freeze-dried and crushed to a powder by using an Automill machine (Tokken, Inc., Chiba, Japan). The PBS solutions including fecal source and the substrate were purged with N_2 gas to allow for any residual oxygen to be displaced from the headspace. The suspensions were incubated at 37 °C under anaerobic conditions in an incubator without shaking. Resazurin remains colourless under anaerobic conditions and turns red in the presence of oxygen, and great care was taken to ensure that the experiments were conducted under anaerobic conditions to prevent the solution turning red. The suspensions were collected after 12 h incubation and then centrifuged. The supernatants of the centrifuged samples were used as samples for NMR measurements. The experiments (i.e., *in vitro* incubation) were performed 3–5 times for each substrate and the control.

2.3. Animal experiments

All animal experiments were approved by the Animal Research Committees of RIKEN Yokohama Research Institute and Yokohama City University. Animals were kept in environmentally controlled animal facilities at the Yokohama City University. All efforts were made to minimise suffering with minimal use of mice. Male 10-week-old BALB/cA mice (CLEA Japan, Inc., Tokyo, Japan) were housed at 23–25 °C and 50–60% relative humidity with a 12 h light-dark cycle. The mice were fed a CLEA Rodent Diet CA-1 (CLEA Japan, Inc., Tokyo, Japan) for 1 week before commencement of experiments. The experimental diet consisted of 5% JBO_{VS} mixed with CLEA Rodent Diet CA-1 (control diet) excluding fibre contents. The mice were fed the experimental diet for a week after a week of the control diet intakes. Thirty-two fecal pellets were collected from the mice. The pellets were lyophilized and then stored at −80 °C.

2.4. NMR spectroscopy

The supernatants of the collected samples from the *in vitro* experiments were suspended in 10% (v/v) deuterium oxide (D_2O) and 1 mM sodium 2,2-dimethyl-2-silapentane-5-sulfonate (DSS) as an internal standard. JBO_{VS} and 32 fecal samples from the *in vivo* experiments were freeze-dried and 50 mg of JBO_{VS} and 5 mg of the freeze-dried fecal samples were extracted with 600 μl of a phosphate buffer solution (0.1 M K_2HPO_4/KH_2PO_4, pH 7.0), containing 90% D_2O and 1 mM DSS at 50 °C for 5 min. After

centrifugation, the extracted supernatant was transferred into a 5 mm ø NMR tube for NMR measurements. All one dimensional (1D) Watergate spectra were acquired at 298 K on a DRX-500 spectrometer (Bruker Biospin, Rheinstetten, Germany) equipped with a ^{1}H inverse triple-resonance probe with triple-axis gradients (Bruker Biospin) as previously described (Date, Iikura, Yamazawa, Moriya, & Kikuchi, 2012). Briefly, 32,768 data points with a spectral width of 12,500 Hz were collected into 32 transients and 1 dummy scan, and residual water signals were suppressed by Watergate pulse sequence with a 1.3-s cycle time. Prior to Fourier transformation, the free induction decays were multiplied by an exponential window function corresponding to a 0.3 Hz line broadening factor. The acquired spectra were manually phased and baseline-corrected. Two dimensional (2D) ^{1}H-^{13}C heteronuclear single quantum coherence (HSQC) spectra and total correlation spectroscopy (TOCSY) were recorded on a Bruker DRU-700 NMR spectrometer equipped with a ^{1}H inverse cryogenically cooled probe with a *z* axis gradient as previously described (Kikuchi & Hirayama, 2007; Sekiyama, Chikayama, & Kikuchi, 2010). The HSQC NMR spectra were acquired in the range of 11.7 to −2.3 ppm in F2 (^{1}H) using 1024 data points and 155–5 ppm in F1 (^{13}C) using 800 data points with 64 scans per F1 increment and an interscan delay (D1) of 2 s with 16 dummy scans. The TOCSY spectra were acquired in the range of 10.7 to −1.7 ppm using 4096 (F2) and 512 (F1) data points with 16 scans and an interscan delay of 2 s with 16 dummy scans. The mixing time (D9) was set to 90 ms. The NMR spectra were processed using NMRPipe software (Delaglio et al., 1995) and assigned using the SpinAssign program from the PRIMe website (Chikayama, Suto, Nishihara, Shinozaki, & Kikuchi, 2008; Chikayama et al., 2010).

For quantification analysis of each sugar component included in JBO_{VS}, we prepared and precisely quantified standard solutions containing known concentrations of each sugar component (i.e., 50, 10, 1.0, and 0.5 mM for glucose and fructose, 10, 1.0, 0.5, and 0.1 mM for sucrose, and 10, 5.0, 1.0, and 0.5 mM for galactose), and used these solutions to construct standard curves for each sugar component. These standard curves were then used to estimate the concentrations of the different components in the JBO_{VS} from the HSQC spectra using the same NMR measurement conditions. The following acquisition NMR parameters were used for the quantification HSQC measurements: the size of fid was 1024 data points in F2 (^{1}H) and 240 data points in F1 (^{13}C), with 40 scans and an interscan delay (D1) of 1.5 s with 16 dummy scans; the transmitter frequency offset was 4.708 ppm in F2 (^{1}H) and 75.5 ppm in F1 (^{13}C) with spectral widths of 14 and 59 ppm in F2 (^{1}H) and F1 (^{13}C), respectively. For the construction of the standard curves, only signals with a coefficient of determination (R^2) greater than 0.999 were selected for each sugar component. Using the resulting standard curves, the sugar concentration estimates were calculated by averaging each signal (excluding any overlapping signals) as well as the standard deviations.

2.5. DNA extraction and PCR-DGGE analysis

Bacterial cell pellets of the collected samples from *in vitro* experiments and the fecal samples from *in vivo* experiments were suspended in TE buffer (10 mM Tris–HCl, 1 mM EDTA, pH 8.0). Then, the samples were homogenised and disrupted with 0.1 mm Zirconia/Silica Beads (BioSpec Products, Inc., OK, USA) and extracted with 10% sodium dodecyl sulphate (SDS)/TE solutions. After centrifugation at 20,000*g* for 10 min at room temperature, the DNA was purified using a phenol/chloroform/isoamyl alcohol (25:24:1) solution and precipitated by adding ethanol and sodium acetate, and then stored at −20 °C.

For PCR-DGGE analyses, PCR amplification and DGGE analysis were performed according to previous studies (Date et al., 2010). The gels obtained from DGGE were stained using SYBR Green I (Lonza, Rockland, ME USA) and were acquired by GelDoc XR (Bio-Rad Laboratories Inc., Tokyo, Japan).

2.6. Phylogenetic analysis

For identification of the bacterial origin of DNA sequences in the gel, selected DGGE bands were excised from the original gels and their DNA fragments were reamplified with the corresponding primers. The obtained PCR product was sequenced using a DNA Sequencer (Applied Biosystems 3130xl Genetic Analyzer) with a BigDye Terminator v3.1 Cycle Sequencing Kit (Applied Biosystems Japan Ltd., Tokyo, Japan). The sequences were submitted to BLAST search programs at the DNA Data Bank of Japan (DDBJ) to determine their closest relatives. The sequences determined in this study and those retrieved from the databases were aligned using CLUSTAL W, and then a phylogenetic tree was constructed with CLUSTAL W and Tree View by the neighbour-joining method.

2.7. Quantification of lactate dehydrogenase genes

Total bacterial RNA was extracted and reverse-transcribed by using RNeasy (QIAGEN K. K., Tokyo, Japan) and RevaTra Ace (TOYOBO Co., Ltd., Osaka, Japan) according to the manufacturer's instructions. Real-time PCR was performed using SYBR Premix Ex Taq™ (Takara Bio Inc., Shiga, Japan) and specific primers targeted for lactate dehydrogenase genes as follows: 5′- cta agg gtg ctg acg gtg tt -3′ (forward) and 5′- agc aat tgc gtc agg aga gt -3′ (reverse); 5′- tgt caa gca tgc caa atc at -3′ (forward) and 5′- cac cct ttg tcc gat cct ta -3′ (reverse); 5′- atg gct act ggt ttc gat gg -3′ (forward) and 5′- atc aag cga agt acc gga tg -3′ (reverse); 5′- cac aag aaa tcg gga tcg tt -3′ (forward) and 5′- aac cag atc agc atc ctt gg -3′ (reverse); and 5′- acc aag aag tta agg aca tgg c -3′ (forward) and 5′- cct tag cga tca ttg ctg aag c -3′ (reverse). These primer sets were referred to in previous reports (Kim, Baek, & Pack, 1991; Smeianov et al., 2007) and designed by ourselves according to a previous study (Date, Isaka, Sumino, Tsuneda, & Inamori, 2008). Assays were performed in triplicate using a Thermal Cycler Dice Real Time System (Takara Bio Inc.).

2.8. ^{1}H NMR imaging

The ^{1}H NMR imaging was performed according to a previous report (Takase et al., 2011) on an NMR spectrometer (500 MHz) equipped with a superconducting magnet (11 T) and an imaging probe (Doty Scientific Inc., Columbia, SC, USA). Briefly, the proton density image technique was set to 0.2 ms of echo time and 1 s of repetition time as the parameters. Both the sampling number and the number of encoding steps were 256. The field of view of the image data was 5 mm^2, and the resolution was 256 pixels per 5 mm. The NMR processing and control software was Delta ver. 4.3-fcll for Linux (JEOL USA, Inc.), and Linux-based ^{1}H NMR data were converted using Analyze^{avw} software (Biomedical Imaging Resource, Mayo Foundation).

2.8. ICP-OES and ICP-MS analysis

Polypropylene products were employed for all test tubes, pipette tips, and syringes. For ICP-OES and ICP-MS analysis, 50 mg of JBO_{VS} were incubated with 2 ml of methanol at 50 °C for 15 min in a Thermomixer comfort (Eppendorf Japan Co., Ltd., Tokyo, Japan) and then centrifuged (17,700*g*, 5 min). The residue was incubated with 2 ml of aqueous nitric acid (6.9% v/v) at 50 °C for 5 min and the supernatant was collected (this step was repeated three times). The combined supernatants (total 6 ml) were filtrated through a Millex GS filter (0.22 μm, Millipore, Billerica, MA, USA) and the filtrate was used for ICP-OES and ICP-MS analysis. ICP-OES and ICP-

MS analysis was performed on a SPS5510 and SPQ9700 (SII Nano-Technology, Chiba, Japan), respectively. The operations of ICP-OES were performed according to a previous study (Sekiyama, Chikayama, & Kikuchi, 2011). The ICP-MS operating conditions were as follows: power 1.4 kW, plasma flow 16.5 l/min, and nebulizer flow 1 l/min.

2.9. Statistical analysis

All 1D ^{1}H NMR data were reduced by subdividing the spectra into sequential 0.04 ppm designated regions between ^{1}H chemical shifts of 0.5–9.0 ppm. After exclusion of the water resonance, each spectrum was normalised by constant sum (Date et al., 2012). The DGGE band signals were calculated by Quantity One software (Bio-Rad Laboratories Inc., Tokyo, Japan). The signal intensities and band position in each lane were divided into a spectrum of 100 variables. Principal component analysis (PCA) was run using R software and performed according to a previous report (Date et al., 2012).

3. Results

3.1. Screening of candidate prebiotic foods by in vitro incubation

The first objective of this study was to develop a rapid and simple method for screening candidate prebiotic foods and their components. In order to develop the screening method, we focused on the metabolic profiles from intestinal microbiota incubated *in vitro* with feces. In our previous study (Date et al., 2010), metabolic dynamics and microbial variability from the *in vitro* incubation with glucose were characteristically observed, and the substrate was completely consumed within 12 h of incubation. In addition, the metabolic dynamics from the *in vitro* incubation with FOS, raffinose, and stachyose (known as prebiotic foods) were characteristically varied in ^{1}H NMR-based metabolic profiles. Therefore, we decided that 12 h after incubation was the best sampling point for evaluation and comparison of metabolic profiles generated by intestinal microbiota incubated with various substrates.

The metabolic profiles from incubation with FOS, raffinose, stachyose, pectin from apple, kelp, wheat-bran, starch from wheat, Japanese mustard spinach, chlorella, glucan, arrowroot, starch from arrowroot, agar, carrageenan, JBO, JBO_{VS}, onion, or control (no addition of substrate) were measured by an NMR-based metabolomics approach (Fig. S1). Plots of PCA scores for these data demonstrated that the metabolic profiles clustered to two groups (Fig. 1A). One group included the metabolic profiles from the incubation with FOS, raffinose, stachyose, JBO, JBO_{VS}, and onion. The other metabolic profiles obtained from the incubation with pectin from apple, kelp, wheat-bran, starch from wheat, Japanese mustard spinach, chlorella, glucan, arrowroot, starch from arrowroot, agar, or carrageenan were clustered with the controls. Because the FOS, raffinose, and stachyose are well known prebiotic foods, JBO, JBO_{VS}, and onion were potential candidate prebiotic foods.

3.2. Identification of key metabolites in the clusterings

To identify the factors contributing to these clusterings, analysis of loading plots based on the ^{1}H NMR spectra was performed to provide information on the spectral position responsible for the position of coordinates in the corresponding scores plots (Fig. 1B). The results indicated that lactate and acetate contributed to the clustering for both the 'candidate prebiotic food group' and the 'control group' because the peaks of acetate and lactate in the 'candidate prebiotic food group' were shifted (Fig. S1). Furthermore, the pH levels were relatively low and the lactate production levels were relatively high in the 'candidate prebiotic food group' compared with the 'control group' (Fig. 1C). In contrast, the relative abundance of acetate was lower in the 'candidate prebiotic food group' compared with the 'control group', and tended to be negatively correlated with a decrease in the pH value, although enhanced acetate levels were observed in all of the substrates following 12 h of incubation (Fig. 1D). These results indicated that the observed peak shifts of acetate and lactate in the 'candidate prebiotic food group' were caused by decreased pH levels with increased lactate production. Furthermore, it is likely that the observed reduction in the pH values was largely dependent on the levels of lactate production in the *in vitro* experiments. Therefore, JBO, JBO_{VS}, and onion influenced the microbial community in the feces during *in vitro* incubation resulting in an increase in the production of lactate and a decrease in the pH level.

3.3. Microbial community analysis

Next, we focused on the microbial community profiles because of different metabolic and pH profiles in the 'candidate prebiotic food group' compared with the 'control group'. In order to compare the microbial communities in the incubated feces, DGGE analysis was performed (Fig. 1E). The three major bands detected by DGGE analysis after incubation indicated the presence of *Lactobacillus johnsonii*, *Lactobacillus murinus*, and *Lactobacillus fermentum*. Surprisingly, these three bacteria all from the *Lactobacillus* group were detected as major bacteria in the microbial communities not only incubated with substrates of the 'candidate prebiotic food group', but also that of the 'control group'. In addition, PCA was used to enable a more detailed comparison of the microbial profiles (i.e., considering the minor population of the microbial communities). The microbial community profiles for the different substrates containing feces prior to the incubation were almost identical and formed a cluster on the PCA score plot, whereas the profiles of the different samples varied considerably after 12 h of incubation (Fig. 1F). The microbial profile of the FOS-treated feces was more similar to those of the control (no addition of substrate) and JBO than the profiles of the Japanese mustard spinach, arrowroot, glucan, and wheat-bran, whereas the profiles of JBO_{VS}-treated feces were intermediate between those of the FOS and Japanese mustard spinach. These results indicated that there were variations in the detailed microbial community profiles (minor population) based on differences in the substrates being incubated, although the major microbes detected by DGGE analysis were almost identical to those of the three bacteria (i.e., *L. johnsonii*, *L. murinus*, and *L. fermentum*), which all belong to the *Lactobacillus* genus, as shown in Fig. 1E. The microbial community profiles were therefore influenced by the *in vitro* incubation process, although minor differences based on fluctuations in the major microbial community were also observed. Nevertheless, since the lactate production levels were high in the 'candidate prebiotic food group' compared with the 'control group', the mRNA from various lactate dehydrogenase genes, which is the key enzyme responsible for lactate production by *Lactobacillus* bacteria, were quantified by quantitative real-time PCR (Fig. 1G). The expression levels of the mRNA in the feces incubated with the JBO_{VS} as a substrate were higher than both the control and the FOS. Therefore, this suggested that the JBO_{VS} modulated the activities of the microbial community, and stimulated the metabolic dynamics of the *Lactobacillus* group to produce the lactate.

3.4. Compositional characterisation of JBO_{VS}

Because the JBO_{VS} was considered a 'candidate prebiotic food', we focused on the JBO_{VS} for further analysis. The VS was initially accumulated in the cavities of young leaves of the JBOs, and was found to be much more abundant during the initial growth stage

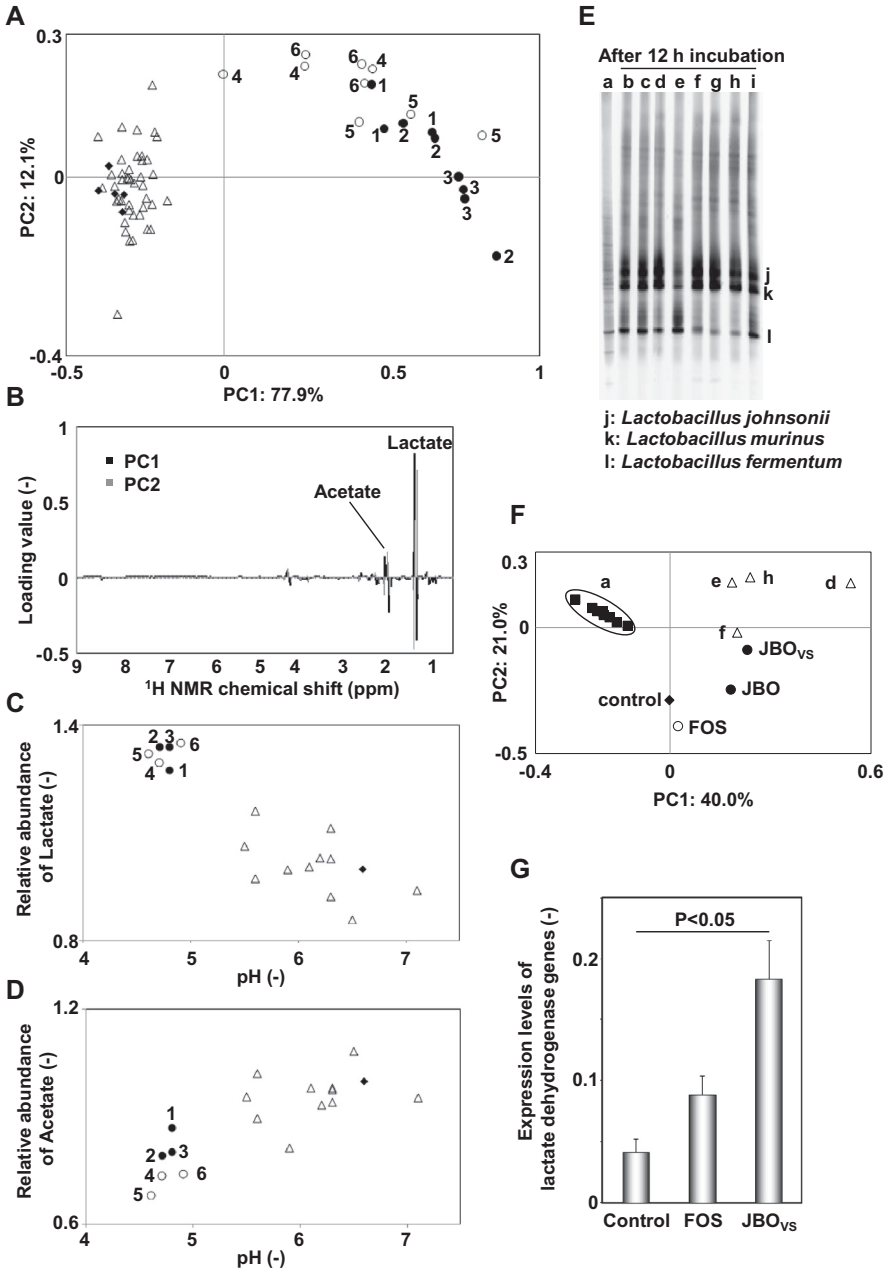

Fig. 1. Characterisation and evaluation of JBO_{VS} by an *in vitro* incubation method. (A) Plot of PCA scores of metabolic profiles based on ^{1}H NMR spectra of the incubated samples. (B) Loading plots of ^{1}H NMR spectra of the incubated samples. (C) Relationship between relative abundance of lactate from ^{1}H NMR spectra and pH. The lactate values were calculated from the ^{1}H NMR spectra in the range of 1.26–1.41 ppm (this range included the peak tops and shoulders taken from the spectra of all of the incubated samples) because the peaks corresponding to the lactate in the 'candidate prebiotic food group' were shifted as a consequence of the reduced pH levels. (D) The relationship between the relative abundance of acetate as determined by ^{1}H NMR and the pH. Note that the acetate values were calculated from the ^{1}H NMR spectra in the range of 1.89–2.04 ppm for the same reason as that described above for the lactate. (E) Microbial community profiles evaluated by DGGE fingerprinting. (F) Microbial community profiles evaluated by PCA. (G) Expression levels of lactate dehydrogenase genes in JBO_{VS} compared with control and fructo-oligosaccharide (FOS). Difference between control and JBO_{VS} was analysed by Student's *t*-test. Closed circles; 1: JBO_{VS}, 2: JBO, 3: onion, open circles; 4: FOS, 5: raffinose, 6: stachyose, open triangles; other foods and their components, and closed diamonds; control, a: feces before incubation, b: JBO_{VS}, c: JBO, d: Japanese mustard spinach, e: arrowroot, f: glucan, g: starch from wheat, h: wheat-bran, i: control, j–l: the positions of detected bands as *Lactobacillus johnsonii* (j), *Lactobacillus murinus* (k), and *Lactobacillus fermentum* (l).

than it was during the mature stage. The formation of cavities in the leaves of the JBOs was necessary for the accumulation of the VS, and the cavities on the leaves were therefore observed by ^{1}H NMR imaging. The cavities of the first leaf, second leaf, and third leaf in JBO were observed at 28, 21, and 36 days after sowing, respectively (Fig. 2A). The outer and inner diameters of the cavity were measured from the observed images (Fig. 2B). The JBO_{VS} accumulated in the cavity of these leaves. In order to characterise the chemical and mineral compositions of the JBO_{VS} collected from the mature growth stage, NMR and ICP-OES/MS analysis were performed. The main chemical components of the JBO_{VS} were detected as D-glucose, D-fructose, D-galactose, sucrose, acetate, malate, trimethylamine (TMA), L-glutamine, L-threonate, and L-serine according to ^{1}H-^{13}C HSQC data assigned using public database we developed on the PRIMe web site and the assignments were confirmed using the TOCSY NMR spectrum (Fig. 2C, Table 1, and Fig. S3). D-Glucose, D-fructose, D-galactose, and sucrose, in particular, were abundantly included in the JBO_{VS}, and these sugar components were quantitatively analysed using the HSQC NMR spectra with the standard curve method. The average values for the differ-

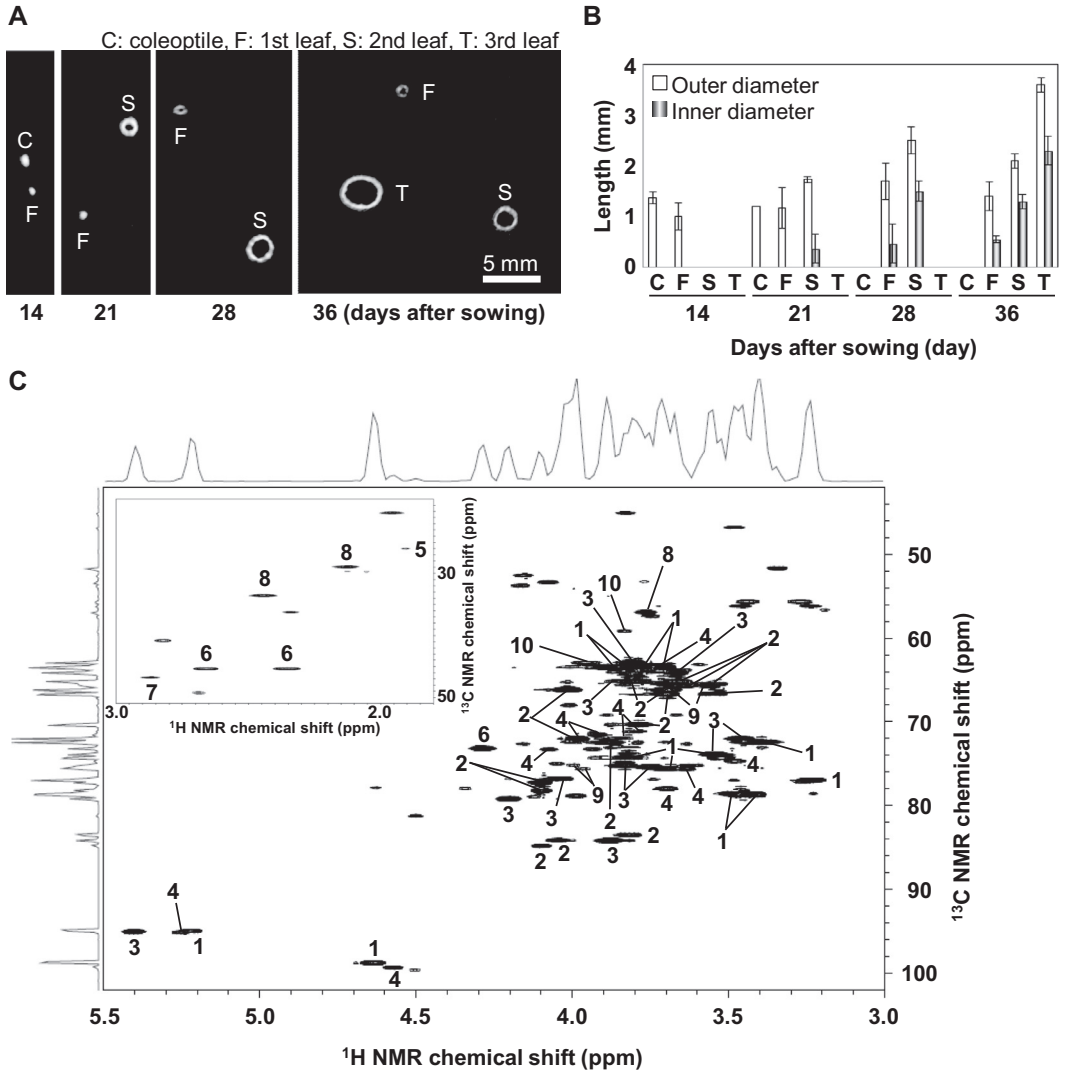

Fig. 2. Characteristics of JBO_{VS}. (A) Images of the cavities in the JBOs at a young growth stage were observed using MRI. C: coleoptile, F: 1st leaf, S: 2nd leaf, T: 3rd leaf. (B) Inner and outer diameter of the cavity in JBO measured using MRI. The error bars represent the standard deviations, which were calculated from the diameters of three JBOs. JBO_{VS} was formed in these cavities. (C) ^{1}H-^{13}C HSQC spectrum for JBO_{VS} collected from the mature growth stage. The region from 3.0 to 5.5 for ^{1}H and from 42 to 102 for ^{13}C is displayed. 1: D-Glucose, 2: D-Fructose, 3: Sucrose, 4: D-Galactose, 5: Acetate, 6: Malate, 7: Trimethylamine (TMA), 8: L-Glutamine, 9: L-Threonate, 10: L-Serine.

ent sugar components in the measured solutions were 26.3 (D-glucose), 24.4 (D-fructose), 2.28 (D-galactose), and 5.66 mM (sucrose), and the values per g-JBO_{VS} were converted as shown in Table 2. These results indicated that D-glucose and D-fructose were the most abundant components in the JBO_{VS}. The sugars (especially, D-glucose and D-fructose) were the most abundant components suggesting that they might exist in the form of oligo- and/or poly-saccharides (i.e., fructose-based carbohydrates) in the JBO_{VS}. Moreover, the JBO_{VS} were composed of many elements such as K, Ca, S, Mg, P, Al, Na, Si, Fe, Sr, B, Mn, Zn, Rb, Sc, Ti, Cu, Ba, V, and Mo according to the ICP-OES/MS data (Table 3 and Fig. S2A).

3.5. Inspection of lactate and acetate production on a host-microbial symbiotic system by JBO_{VS} intake

The expected effects of JBO_{VS} on the host-microbial symbiotic system in mice were deduced from the metabolic profiles of the 32 fecal samples measured by NMR spectroscopy. Plots of PCA scores for the ^{1}H NMR spectra demonstrated that the metabolic profiles clustered according to the differences between the control and JBO_{VS} diet intake (Fig. 3A). The relative intensities of lactate and acetate in the JBO_{VS} diet intake were significantly higher compared with those in the control diet intake (Fig. 3B). Therefore, intake of the JBO_{VS} was likely to be accompanied by increases in the production levels of lactate and acetate in the mouse intestines. In addition, to investigate the effects of JBO_{VS} on the intestinal microbiota in mice, the microbial community profiles in the fecal samples were analysed by DGGE fingerprinting. Nine predominant bands were observed. To obtain more definitive information regarding the taxonomy of these major bands, a phylogenetic tree was constructed based on the 16S rRNA gene fragments derived from the DGGE gel bands (Fig. S4). DNA sequences from bands 1 to 7 were categorised in the phylum Firmicutes, and those from bands 8 to 9 were categorised in the phylum Bacteroidetes (Fig. S4). Plots of PCA scores for DGGE fingerprinting data demonstrated that the microbial community profiles clustered according to the differences between the control and JBO_{VS} diet intake (Fig. 3C). Bacteria originating from bands 4, 5, and 8 were related to *L. murinus* and belonged to the *Bacteroidetes* sp. group which contributed to the separation in the JBO_{VS} diet intake compared with control diet intake results (Fig. 3D). These three bacteria were significantly increased in the animals fed the JBO_{VS} diet intake compared with those fed the control diet (Fig. 3D).

Table 1
JBO_{VS} components detected by ^{1}H-^{13}C HSQC NMR measurements.

Number	Metabolite	Peak detected in HSQC spectra		Database peak (PRIMe web site)	
		^{1}H NMR chemical shift (ppm)	^{13}C NMR chemical shift (ppm)	^{1}H NMR chemical shift (ppm)	^{13}C NMR chemical shift (ppm)
1	D-Glucose	3.229	76.958	3.235	76.826
1	D-Glucose	3.393	72.416	3.399	72.292
1	D-Glucose	3.448	78.716	3.452	78.652
1	D-Glucose	3.475	78.569	3.474	78.487
1	D-Glucose	3.516	74.316	3.526	74.162
1	D-Glucose	3.704	75.491	3.706	75.498
1	D-Glucose	3.707	63.480	3.715	63.447
1	D-Glucose	3.748	63.334	3.762	63.287
1	D-Glucose	3.817	74.177	3.823	74.163
1	D-Glucose	3.831	63.330	3.828	63.287
1	D-Glucose	3.885	63.477	3.887	63.446
1	D-Glucose	4.637	98.777	4.639	98.620
1	D-Glucose	5.225	94.836	5.225	94.803
2	D-Fructose	3.543	66.703	3.555	66.631
2	D-Fructose	3.571	65.388	3.567	65.467
2	D-Fructose	3.639	65.678	3.648	65.718
2	D-Fructose	3.667	65.094	3.667	65.088
2	D-Fructose	3.694	66.106	3.694	66.068
2	D-Fructose	3.694	66.548	3.705	66.625
2	D-Fructose	3.803	65.086	3.792	65.099
2	D-Fructose	3.789	70.364	3.792	70.306
2	D-Fructose	3.817	83.402	3.818	83.339
2	D-Fructose	3.885	72.417	3.885	72.439
2	D-Fructose	3.981	71.976	3.990	71.938
2	D-Fructose	4.008	66.116	4.012	66.022
2	D-Fructose	4.049	84.131	4.038	83.961
2	D-Fructose	4.104	84.723	4.103	84.745
2	D-Fructose	4.104	77.253	4.105	77.173
2	D-Fructose	4.104	78.133	4.104	78.143
3	Sucrose	3.461	71.978	3.458	71.859
3	Sucrose	3.543	73.877	3.544	73.782
3	Sucrose	3.667	64.065	3.666	63.977
3	Sucrose	3.748	75.347	3.747	75.189
3	Sucrose	3.807	62.823	3.802	62.786
3	Sucrose	3.816	65.094	3.808	65.024
3	Sucrose	3.830	75.200	3.833	75.089
3	Sucrose	3.885	84.137	3.880	84.080
3	Sucrose	4.036	76.813	4.036	76.688
3	Sucrose	4.200	79.155	4.208	79.080
3	Sucrose	5.403	94.978	5.397	94.813
4	D-Galactose	3.475	74.614	3.478	74.665
4	D-Galactose	3.639	75.639	3.636	75.487
4	D-Galactose	3.694	77.984	3.694	77.896
4	D-Galactose	3.737	63.762	3.735	63.829
4	D-Galactose	3.803	71.099	3.797	71.064
4	D-Galactose	3.844	71.976	3.833	71.832
4	D-Galactose	3.912	71.535	3.918	71.441
4	D-Galactose	3.995	72.270	3.977	72.032
4	D-Galactose	4.077	73.297	4.076	73.247
4	D-Galactose	4.569	99.225	4.572	99.180
4	D-Galactose	5.253	95.122	5.252	95.012
5	Acetate	1.902	25.979	1.900	26.000
6	Malate	2.353	45.317	2.349	45.192
6	Malate	2.659	45.322	2.661	45.184
6	Malate	4.282	73.146	4.290	72.953
7	Trimethylamine	2.873	46.780	2.870	47.320
8	L-Glutamine	2.134	28.940	2.130	28.952
8	L-Glutamine	2.448	33.500	2.444	33.579
8	L-Glutamine	3.762	56.882	3.763	56.840
9	Threonate	3.613	65.502	3.608	65.514
9	Threonate	3.967	75.629	3.969	75.313
9	Threonate	3.673	65.690	3.676	65.522
9	Threonate	3.994	75.189	3.988	75.110

(*continued on next page*)

Table 1 (*continued*)

Number	Metabolite	Peak detected in HSQC spectra		Database peak (PRIMe web site)	
		^{1}H NMR chemical shift (ppm)	^{13}C NMR chemical shift (ppm)	^{1}H NMR chemical shift (ppm)	^{13}C NMR chemical shift (ppm)
10	L-Serine	3.830	59.088	3.828	59.116
10	L-Serine	3.954	62.896	3.954	62.939

Table 2
Quantification values of each sugar components in JBO_{VS}.

Metabolite	Concentration (mg/g-VS)	Standard deviation
D-Glucose	157.6	±3.93
D-Fructose	146.5	±3.68
Sucrose	64.6	±1.11
D-Galactose	13.7	±1.41

Table 3
Minerals detected in JBO_{VS}.

Element	Equipment	Concentration		Content rate (%)
K	ICP-OES	10.2	mg/g-VS	52.52
Ca	ICP-OES	5.47	mg/g-VS	28.23
S	ICP-OES	1.71	mg/g-VS	8.81
Mg	ICP-OES	1.42	mg/g-VS	7.31
P	ICP-OES	349.2	μg/g-VS	1.80
Al	ICP-MS	72.1	μg/g-VS	0.37
Na	ICP-OES	32.4	μg/g-VS	0.17
Si	ICP-OES	31.4	μg/g-VS	0.16
Fe	ICP-OES	30.3	μg/g-VS	0.16
Sr	ICP-MS	19.7	μg/g-VS	0.10
B	ICP-MS	18.5	μg/g-VS	0.10
Mn	ICP-MS	17.4	μg/g-VS	0.09
Zn	ICP-MS	14.3	μg/g-VS	0.07
Rb	ICP-MS	6.85	μg/g-VS	0.04
Sc	ICP-MS	3.60	μg/g-VS	0.02
Ti	ICP-OES	3.28	μg/g-VS	0.02
Cu	ICP-MS	3.23	μg/g-VS	0.02
Ba	ICP-MS	1.39	μg/g-VS	0.01
V	ICP-MS	0.20	μg/g-VS	0.00
Mo	ICP-MS	0.14	μg/g-VS	0.00

4. Discussion

This study focused on a rapid and simple method for screening candidate prebiotic foods and their components. The JBO_{VS} was identified as one of the candidate prebiotic foods. The JBO_{VS} accumulated in the cavity of the leaf was primarily composed of sugar components, especially fructose-based carbohydrates. The fructose-based carbohydrates are well-known to influence the intestinal microbiota, and the basis of *Bacteroides* spp. proliferation in response to fructose-based carbohydrates is known (Sonnenburg et al., 2010). In addition, the fructose-based carbohydrates derived from plants such as Chinese yam and Chinese bitter melon as well as JBO_{VS} have attracted attention as prebiotic foods, and were reported to promote the growth of helpful intestinal microbiota such as *Bacteroides* spp. who are capable of utilizing nearly all of the major plant and host glycans (Hvistendahl, 2012; Martens et al., 2011). The fructose-based carbohydrates activate certain bifidobacterial strains encoded by the genes of the ATP-binding-cassette-type carbohydrate transporter, promote acetate production in the intestines, and enhance the barrier function of the intestines and host immune systems (Fukuda et al., 2011). This promotion of acetate production is consistent with our results from *in vivo* experiments. Therefore, the JBO_{VS} may promote the growth of helpful intestinal microbiota, enhance the barrier function of the intestines for maintenance of host homeostasis, and be regarded as a potential prebiotic food. In addition, to our knowledge, this study is the first report to characterise the chemical compositions of JBO_{VS}.

The *in vitro* incubation with JBO_{VS} influenced the microbial community in the feces accompanied by an increase in the production level of lactate and a decrease in the pH level. This result was consistent with the observed increase in the production levels of lactate in the mice intestines after ingestion of the JBO_{VS}. Therefore, JBO_{VS} was likely to cause a similar fluctuation of metabolic dynamics in the microbial community both *in vitro* and *in vivo*. Moreover, our results revealed that ingestion of JBO_{VS} contributed to lactate and acetate production in the intestinal microbiota. In contrast, an increased population of bacteria related to *L. murinus* and belonging to the *Bacteroidetes* sp. group was influenced by the intake of JBO_{VS} into the host-microbial symbiotic systems. This *in vivo* observation was somewhat different to the observed increased population of bacteria related to *L. johnsonii*, *L. murinus*, and *L. fermentum* found in the *in vitro* experiment. This small difference was considered a bias brought about by the *in vitro* incubation because the environmental factors for growth, metabolism, and interactions of microbiota were considerably different compared with the *in vivo* conditions. Taken together, the *in vitro* and *in vivo* metabolic profiling results were similar whereas the *in vitro* and *in vivo* microbial community profiling showed some variability. Therefore, metabolic profiling by *in vitro* methods may offer a practical approach for easy screening to measure the metabolic endpoints that link directly to whole system activity and are determined by both microbial ecosystems and environmental factors. In addition, lactate and acetate may be considered as useful biomarkers for *in vitro* screening because they correlate tightly with intestinal microbiota and host cells and several beneficial effects for human health were reported (Fukuda et al., 2011; Okada et al., 2013).

According to our *in vivo* observations, increases in the *L. murinus* and *Bacteroidetes* sp. populations and acetate and lactate production levels in the intestine were the result of the effects to the intestinal microbiota and host-microbial co-metabolic process. Acetate has been reported to show anti-inflammatory properties (Fukuda et al., 2011), which are derived by colonic bacteria after fermentation of dietary carbohydrates. Moreover, acetate has been reported to bind and activate the G-protein-coupled receptor GPR43, and stimulation of GPR43 by short-chain fatty acids including acetate is necessary for the normal resolution of certain immune and inflammatory responses (Maslowski et al., 2009). Therefore, acetate is considered to play an important role in the maintenance of homeostasis in host-microbial ecosystems. Furthermore, it was reported that bacteria from the Bacteroidetes phylum produce high levels of acetate and propionate (Macfarlane & Macfarlane, 2003), suggesting that the *Bacteroidetes* sp. detected in the DGGE analysis and the increase of this population in the JBO_{VS} diet intake group was related to the acetate production process in the intestines. In addition, members of the genus *Lactobacillus* including *L. murinus*, which is well known to produce lactate, are predominant inhabitants of the intestinal tract of mammals, where they are thought to play an important role in the maintenance of colonisation resistance and prevention of overgrowth of enteric pathogens (Okada et al., 2013). In addition, a recent study reported the increase in live *L. murinus* and lactate production was enhanced epithelial cell proliferation (Okada et al., 2013).

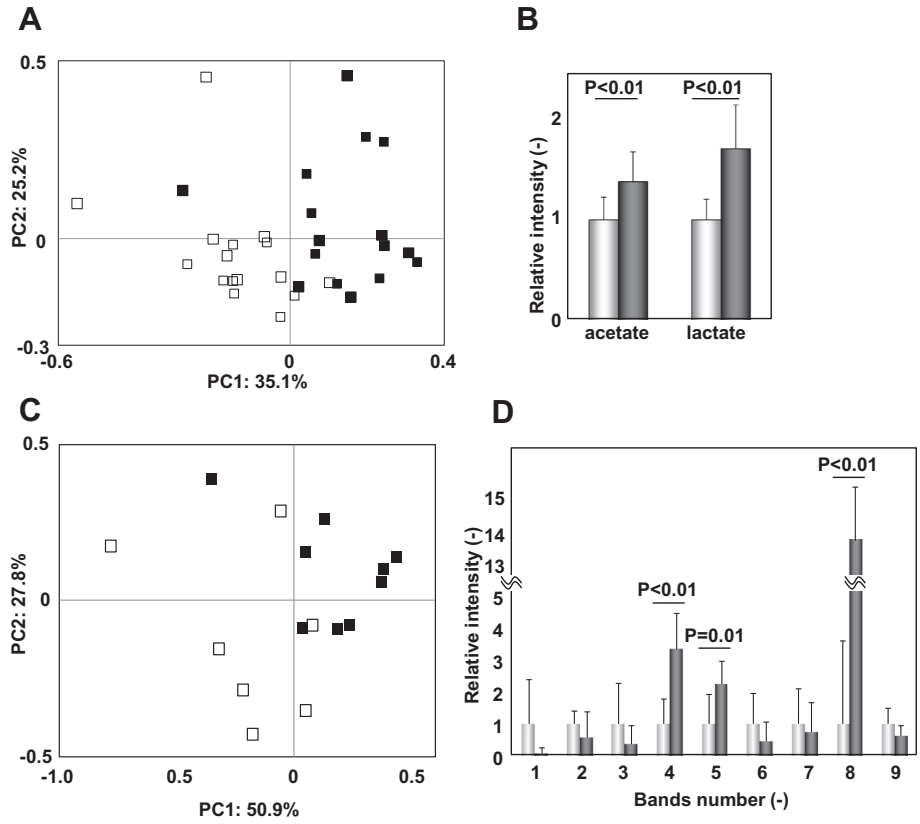

Fig. 3. Metabolic and microbial community profiles based on ^{1}H NMR spectra and DGGE fingerprinting of fecal samples from mice, respectively. (A) Plot of PCA scores of NMR profiles. The data points were separated by the differences between control diet (open square) and JBO_{VS} diet (closed square) intake. (B) The average intensities of acetate and lactate for control (white) and JBO_{VS} (black) diet intake were shown. (C) Plot of PCA scores on DGGE profiles. The data points were likely to be separated by the differences between the control diet (open square) and JBO_{VS} diet (closed square) intake. (D) The average intensities of each band based on DGGE data for control (white) and JBO_{VS} (black) diet intake were shown. Differences between two groups were analysed by Student's *t*-test.

Therefore, it was suggested that the increase in *L. murinus* in the JBO_{VS} diet intake group was related to the lactate production in our *in vivo* experiments. Taken together, the effect of JBO_{VS} on the intestinal environment was to increase the production and population levels of these metabolites and bacteria, which in turn, might improve the intestinal immunity and contribute to the maintenance of homeostasis in the host-microbial ecosystem.

This study identified JBO_{VS} as a candidate prebiotic food by an *in vitro* screening method. The approach described herein should be useful as a screen for potential prebiotic foods and for estimating the effects of foods and their components on host-microbial symbiotic ecosystems. Although the mechanisms responsible for the JBO_{VS} benefits remain largely unclear, our preliminary data suggested that the systemic effects on mice were observed as increases in potassium, boron, ethanolamine, and *N*-acetyl-D-glycoprotein levels in excreted urine, and decreases in succinate, creatine, and hypotaurine levels in excreted urine (Figs. S5–S7 and Text S1). Future work will provide important information about the systemic and targeted effects of candidate prebiotic foods screened by our *in vitro* evaluation method on host-microbial symbiotic systems in mammals including human, and should serve as a useful diagnostic for personal and public health purposes.

5. Conclusion

In this study, we performed an *in vitro* evaluation method using the metabolic dynamics of microbial community as an indicator for screening candidate prebiotic foods. The JBO_{VS}, JBO, and onion were nominated as candidate prebiotic foods. In addition, characterisation of chemical and mineral compositions in the JBO_{VS} revealed that sugar components, especially fructose-based carbohydrates were present in significant quantities in the JBO_{VS}. Furthermore, validation of the effects of the JBO_{VS} intake on mice was observed as increases in the *L. murinus* and *Bacteroidetes* sp. populations and acetate and lactate production levels in the intestine, which was largely consistent with the results from our *in vitro* incubation method. Our *in vitro* evaluation approach should be useful as a rapid and simple screening tool for potential prebiotic foods.

Acknowledgements

The authors wish to thank Eisuke Chikayama, Yuuri Tsuboi, Amiu shino, Makiko Akama, Keiko Komatsu (RIKEN), and Tatsuki Ogura (Yokohama City University) for stimulating discussion, technical assistance, and useful advice on NMR measurements and analysis. The authors would like to thank Takeo Kitaura (Kanagawa Agricultural Technology Center) for growing Japanese bunching onions. This research was supported in part by Grants-in-Aid for Scientific Research (C) (J.K.) from the Ministry of Education, Culture, Sports, Science, and Technology, Japan.

Appendix A. Supplementary data

Supplementary data associated with this article can be found, in the online version, at http://dx.doi.org/10.1016/j.foodchem.2013.11.126.

References

Chikayama, E., Sekiyama, Y., Okamoto, M., Nakanishi, Y., Tsuboi, Y., Akiyama, K., et al. (2010). Statistical indices for simultaneous large-scale metabolite detections for a single NMR spectrum. *Analytical Chemistry, 82*(5), 1653–1658.

Chikayama, E., Suto, M., Nishihara, T., Shinozaki, K., & Kikuchi, J. (2008). Systematic NMR analysis of stable isotope labeled metabolite mixtures in plant and animal systems: coarse grained views of metabolic pathways. *PLoS one, 3*(11), e3805.

Date, Y., Iikura, T., Yamazawa, A., Moriya, S., & Kikuchi, J. (2012). Metabolic sequences of anaerobic fermentation on glucose-based feeding substrates based on correlation analyses of microbial and metabolite profiling. *Journal of Proteome Research, 11*(12), 5602–5610.

Date, Y., Isaka, K., Sumino, T., Tsuneda, S., & Inamori, Y. (2008). Microbial community of anammox bacteria immobilized in polyethylene glycol gel carrier. *Water Science and Technology: A Journal of the International Association on Water Pollution Research, 58*(5), 1121–1128.

Date, Y., Nakanishi, Y., Fukuda, S., Kato, T., Tsuneda, S., Ohno, H., et al. (2010). New monitoring approach for metabolic dynamics in microbial ecosystems using stable-isotope-labeling technologies. *Journal of Bioscience and Bioengineering, 110*(1), 87–93.

Delaglio, F., Grzesiek, S., Vuister, G. W., Zhu, G., Pfeifer, J., & Bax, A. (1995). Nmrpipe – A multidimensional spectral processing system based on unix pipes. *Journal of Biomolecular NMR, 6*(3), 277–293.

Flint, H. J., Bayer, E. A., Rincon, M. T., Lamed, R., & White, B. A. (2008). Polysaccharide utilization by gut bacteria: potential for new insights from genomic analysis. *Nature Reviews Microbiology, 6*(2), 121–131.

Fukuda, S., Toh, H., Hase, K., Oshima, K., Nakanishi, Y., Yoshimura, K., et al. (2011). Bifidobacteria can protect from enteropathogenic infection through production of acetate. *Nature, 469*(7331), 543–547.

Hvistendahl, M. (2012). My microbiome and me. *Science, 336*(6086), 1248–1250.

Kang, M. J., Kim, J. H., Choi, H. N., Kim, M. J., Han, J. H., Lee, J. H., et al. (2010). Hypoglycemic effects of Welsh onion in an animal model of diabetes mellitus. *Nutrition Research and Practice, 4*(6), 486–491.

Kikuchi, J., & Hirayama, T. (2007). Practical aspects of uniform stable isotope labeling of higher plants for heteronuclear NMR-based metabolomics. *Methods in Molecular Biology, 358*, 273–286.

Kim, S. M. F., Baek, S. J., & Pack, M. Y. (1991). Cloning and nucleotide-sequence of the lactobacillus-casei lactate-dehydrogenase gene. *Applied and Environmental Microbiology, 57*(8), 2413–2417.

Lee, J. B., Miyake, S., Umetsu, R., Hayashi, K., Chijimatsu, T., & Hayashi, T. (2012). Anti-influenza A virus effects of fructan from Welsh onion (*Allium fistulosum* L.). *Food Chemistry, 134*(4), 2164–2168.

Li, M., Wang, B., Zhang, M., Rantalainen, M., Wang, S., Zhou, H., et al. (2008). Symbiotic gut microbes modulate human metabolic phenotypes. *Proceedings of the National Academy of Sciences of the United States of America, 105*(6), 2117–2122.

Macfarlane, S., & Macfarlane, G. T. (2003). Regulation of short-chain fatty acid production. *The Proceedings of the Nutrition Society, 62*(1), 67–72.

Martens, E. C., Lowe, E. C., Chiang, H., Pudlo, N. A., Wu, M., McNulty, N. P., et al. (2011). Recognition and degradation of plant cell wall polysaccharides by two human gut symbionts. *PLos Biology, 9*(12).

Maslowski, K. M., Vieira, A. T., Ng, A., Kranich, J., Sierro, F., Yu, D., et al. (2009). Regulation of inflammatory responses by gut microbiota and chemoattractant receptor GPR43. *Nature, 461*(7268), 1282–1286.

Nicholson, J. K., Holmes, E., & Wilson, I. D. (2005). Gut microorganisms, mammalian metabolism and personalized health care. *Nature Reviews Microbiology, 3*(5), 431–438.

Okada, T., Fukuda, S., Hase, K., Nishiumi, S., Izumi, Y., Yoshida, M., et al. (2013). Microbiota-derived lactate accelerates colon epithelial cell turnover in starvation-refed mice. *Nature Communications, 4*, 1654.

Rezzi, S., Ramadan, Z., Fay, L. B., & Kochhar, S. (2007). Nutritional metabonomics: Applications and perspectives. *Journal of Proteome Research, 6*(2), 513–525.

Saulnier, D. M., Spinler, J. K., Gibson, G. R., & Versalovic, J. (2009). Mechanisms of probiosis and prebiosis: considerations for enhanced functional foods. *Current Opinion in Biotechnology, 20*(2), 135–141.

Sekiyama, Y., Chikayama, E., & Kikuchi, J. (2010). Profiling polar and semipolar plant metabolites throughout extraction processes using a combined solution-state and high-resolution magic angle spinning NMR approach. *Analytical Chemistry, 82*(5), 1643–1652.

Sekiyama, Y., Chikayama, E., & Kikuchi, J. (2011). Evaluation of a semipolar solvent system as a step toward heteronuclear multidimensional NMR-based metabolomics for 13C-labeled bacteria, plants, and animals. *Analytical Chemistry, 83*(3), 719–726.

Smeianov, V. V., Wechter, P., Broadbent, J. R., Hughes, J. E., Rodriguez, B. T., Christensen, T. K., et al. (2007). Comparative high-density microarray analysis of gene expression during growth of Lactobacillus helveticus in milk versus rich culture medium. *Applied and Environmental Microbiology, 73*(8), 2661–2672.

Sonnenburg, E. D., Zheng, H. J., Joglekar, P., Higginbottom, S. K., Firbank, S. J., Bolam, D. N., et al. (2010). Specificity of polysaccharide use in intestinal bacteroides species determines diet-induced microbiota alterations. *Cell, 141*(7), 1241–1256.

Takase, T., Ishikawa, H., Murakami, H., Kikuchi, J., Sato-Nara, K., & Suzuki, H. (2011). The circadian clock modulates water dynamics and aquaporin expression in Arabidopsis roots. *Plant & Cell Physiology, 52*(2), 373–383.

Turnbaugh, P. J., Ley, R. E., Hamady, M., Fraser-Liggett, C. M., Knight, R., & Gordon, J. I. (2007). The human microbiome project. *Nature, 449*(7164), 804–810.

Ventura, M., O'Flaherty, S., Claesson, M. J., Turroni, F., Klaenhammer, T. R., van Sinderen, D., et al. (2009). Genome-scale analyses of health-promoting bacteria: probiogenomics. *Nature Reviews Microbiology, 7*(1), 61–71.

Yamamoto, Y., Aoyama, S., Hamaguchi, N., & Rhi, G. S. (2005). Antioxidative and antihypertensive effects of Welsh onion on rats fed with a high-fat high-sucrose diet. *Bioscience, Biotechnology, and Biochemistry, 69*(7), 1311–1317.

Yamamoto, Y., & Yasuoka, A. (2010). Welsh onion attenuates hyperlipidemia in rats fed on high-fat high-sucrose diet. *Bioscience, Biotechnology, and Biochemistry, 74*(2), 402–404.